Journal of Molecular Structure 1140 (2017) 106–112

Contents lists available at ScienceDirect

Journal of Molecular Structure

journal homepage: http://www.elsevier.com/locate/molstruc

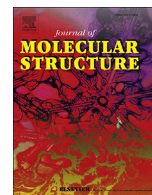

FTIR spectroscopic studies of selenite reduction by cells of the rhizobacterium *Azospirillum brasilense* Sp7 and the formation of selenium nanoparticles

Alexander A. Kamnev*, Polina V. Mamchenkova, Yulia A. Dyatlova, Anna V. Tugarova**

Laboratory of Biochemistry, Institute of Biochemistry and Physiology of Plants and Microorganisms, Russian Academy of Sciences, 13 Prosp. Entuziastov, 410049, Saratov, Russia

A R T I C L E I N F O

Article history:
Received 6 September 2016
Received in revised form
28 November 2016
Accepted 2 December 2016
Available online 2 December 2016

Keywords:
Bacterial selenite reduction
Selenium nanoparticles
FTIR spectroscopy
Transmission electron microscopy (TEM)
Azospirillum brasilense

A B S T R A C T

Microbially driven reduction of selenium oxyanions to elementary selenium, often in the form of nanoparticles (NPs), is widespread in nature. A diversity of possible applications of such biogenic NPs, including those in nanobiotechnology, as well as the specificity of methodologies and mechanisms of their formation via “green synthesis” are very attractive features justifying further studies of the processes of selenium oxyanion bioreduction and the resulting Se^0 nanostructures. In this study, live biomass of the rhizobacterium *Azospirillum brasilense* Sp7 (harvested after the logarithmic growth phase and washed from culture medium components) was used to obtain extracellular Se NPs relatively homogeneous in size (with average diameters within 50–100 nm) in the process of selenite reduction. Both the control cultures of *A. brasilense* Sp7 and those incubated with SeO_3^{2-} (producing Se NPs), as well as the resulting separated Se NPs were studied using Fourier transform infrared (FTIR) spectroscopy in the transmission mode (measured as dried layers on a ZnSe disc), in addition to transmission electron microscopy (TEM), to compare metabolic changes in cells and the bioorganic layers associated with the Se NPs. In the control culture (stored for 24 h in physiological saline), FTIR spectroscopic signs of poly-3-hydroxybutyrate (a ‘reserve’ biopolyester) were observed as a response to the lack of nutrients (trophic stress), whereas they were virtually absent in cells incubated for 24 h in physiological saline with 10 mM SeO_3^{2-} (toxicity stress). FTIR spectra of Se NPs separated from bacterial cells showed bands typical of proteins, polysaccharides and lipids associated with the particles (in line with their TEM images showing a thin layer over the NPs), in addition to strong carboxylate bands, which evidently stabilise the NP structure and morphology.

© 2016 Elsevier B.V. All rights reserved.

1. Introduction

Biogenic formation of various nanostructured materials by live microorganisms, which is widespread in nature, has been increasingly attracting the attention of researchers over the last decade [1–5]. This is both due to a range of diverse applications of such nanoparticles (NPs), including those in nanobiotechnology [4–10], and because of the specificity of methodologies and mechanisms of NPs' formation via “green synthesis” [1–5]. Moreover, detailed knowledge of the related processes can provide biogeochemical evidence for the formation of some mineral deposits (such as gold nuggets) or biotechnological bases in developing bioremediation (phytoremediation) strategies for cleanup of polluted territories involving rhizospheric and soil bacteria [8,11–13].

Recently [14], we demonstrated that *Azospirillum brasilense* (strains Sp245 and Sp7), a ubiquitous most widely studied phytostimulating rhizobacterium of the genus *Azospirillum* [15–17], can reduce selenite (SeO_3^{2-}) to red elementary selenium (Se^0) in the form of NPs (nanospheres, 50–400 nm in size). (It has to be noted that not all microorganisms, which can reduce selenite (Se^{IV}) or selenate (Se^{VI}) to insoluble and, therefore, non-toxic Se^0, produce elementary Se^0 in the form of NPs; the latter may be formed both within the bacterial cells and/or extracellularly [4,5,18–20].) Along with transmission electron microscopy (TEM) images of Se NPs

* Corresponding author.
** Corresponding author.
E-mail addresses: aakamnev@ibppm.ru, a.a.kamnev@mail.ru (A.A. Kamnev), tugarova_anna@mail.ru (A.V. Tugarova).

http://dx.doi.org/10.1016/j.molstruc.2016.12.003
0022-2860/© 2016 Elsevier B.V. All rights reserved.

associated with bacterial cells, their chemical nature and location were elucidated by means of X-ray fluorescence analysis (XFA) and electron energy loss spectroscopy (EELS) [18].

In this work, in which the conditions of Se NPs synthesis by *A. brasilense* (strain Sp7) were further optimised to obtain extracellular Se NPs more homogeneous in size, the bacterial biomass and the resulting isolated Se NPs were comparatively characterised by Fourier transform infrared (FTIR) spectroscopy and TEM. The application of FTIR spectroscopy to studying the resulting biogenic Se NPs is particularly aimed at elucidating their surface biomolecular composition. The latter, according to the literature, may include surface-associated biomacromolecules of microbial origin and bacterial growth medium components which stabilise Se nanospheres [19,20].

2. Materials and methods

2.1. Bacterial strain and growth conditions

Wild-type strain *A. brasilense* Sp7 [21] (ATCC 29145 [22]) was taken from The Collection of Rhizosphere Microorganisms [WDCM 1021] maintained at the Institute of Biochemistry and Physiology of Plants and Microorganisms, Russian Academy of Sciences, Saratov, Russia. Bacteria were cultivated in a liquid modified malate salt medium (MSM) [23] which contained the following salts ($g \cdot l^{-1}$): K_2HPO_4, 3.0; KH_2PO_4, 2.0; NH_4Cl, 0.5; NaCl, 0.1; $FeSO_4 \cdot 7H_2O$, 0.02 (added as chelate with nitrilotriacetic acid); $CaCl_2$, 0.02; $MgSO_4 \cdot 7H_2O$, 0.2; $Na_2MoO_4 \cdot 2H_2O$, 0.002; sodium malate, 5.0 (obtained by mixing 3.76 g of malic acid with 2.24 g NaOH per litre), pH 6.8–7.0.

The culture (volume 100 ml in 250-ml Erlenmeyer flasks) was grown under aerobic conditions on a shaker (180 rpm) for up to 19 h, which corresponds to the end of the logarithmic and the beginning of the stationary growth phase for azospirilla in the MSM under these conditions [18]. Cell growth was monitored at $\lambda = 595$ nm (Spekol 221, Germany); the optical density (A_{595}) values of the resulting culture suspensions were about 1.0–1.3.

2.2. Bacterial synthesis of Se NPs and their purification

All the next steps were performed under sterile conditions. Bacterial cells were harvested by centrifugation in 2-ml Eppendorf tubes (Minispin centrifuge; 15 min, 7000×*g*) and washed three times with sterile saline solution (0.85% NaCl aqueous solution) to remove the culture medium components. The resulting wet biomass pellet was resuspended in half of the initial volume of sterile saline solution. Sodium selenite ($Na_2SeO_3 \cdot 5H_2O$, "Merck") as 0.5 M stock aqueous solution was added to the suspensions up to 10 mM. Suspensions containing the cells (washed as above) and selenite were placed in a thermostat (at 31–32°C). The culture of the same cell density without sodium selenite was used as a control. The process of SeO_3^{2-} reduction was monitored by colour change of the bacterial suspension from colourless to reddish [18]. The SeNPs formed thereby and their localisation were monitored by transmission electron microscopy (TEM; see below).

After 24 h, the bacterial cells were removed from the suspension by 'soft' centrifugation (1400×*g*, 5 min); the supernatant with Se NPs was collected and filtered through a 0.22 or 0.44 μm PVDF filter to remove occasional bacterial cells. The suspensions of Se NPs were further centrifuged at 12000×*g* for 30 min, and the collected precipitate pellet was resuspended in a minimum volume of MilliQ water. The Se NPs obtained were characterised by TEM and FTIR spectroscopy (see below).

2.3. Transmission electron microscopy (TEM)

The samples of bacterial cells or Se NPs (obtained as described above) were placed onto nickel or copper grids coated with formvar (1% formvar in dichloroethane). TEM images were registered on a Libra-120 transmission electron microscope (Carl Zeiss, Jena, Germany).

2.4. Fourier transform infrared (FTIR) spectroscopy

The bacterial aqueous suspensions of *A. brasilense* Sp7 with 10 mM of Na_2SeO_3 were used for Se NPs synthesis (see above). A similarly obtained bacterial aqueous suspension without Na_2SeO_3 was used as a control. To perform FTIR spectroscopic measurements, the samples of bacterial cells (after incubation for 24 h at 31 °C) were collected by centrifugation (7000×*g*, 10 min) and dried (in Eppendorf tubes opened after centrifugation and removal of the supernatant liquid) in a thermostatted desiccator at 45 °C up to a constant weight. Then the dried biomass from each Eppendorf tube was finely powdered in a small agate mortar and resuspended in a small volume of MilliQ water. For transmission FTIR measurements, the resulting aqueous suspensions of bacterial cells (or of Se NPs isolated and purified as described above) were placed as thin films on clean flat ZnSe discs (CVD-ZnSe, "R'AIN Optics", Dzerzhinsk, Russia; diameter 2.5 cm, thickness 0.2 cm) and dried at 45 °C again as described above.

Infrared spectroscopic measurements were performed on a Nicolet 6700 FTIR spectrometer (Thermo Electron Corporation, USA; DTGS detector; KBr beamsplitter). Spectra were collected in the transmission mode with a total of 64 scans (resolution 2 cm^{-1}) against the ZnSe disc background and manipulated using the OMNIC (version 8.2.0.387) software supplied by the manufacturer of the spectrometer. All spectra were smoothed using the standard "automatic smooth" function of the software which uses the Savitsky–Golay algorithm (95-point moving second-degree polynomial), and then the baseline was corrected using the "automatic baseline correct" function. All the FTIR spectroscopic measurements were repeated two or three times for each sample and were well reproducible.

3. Results and discussion

In this work, the methodology for obtaining Se NPs via selenite reduction by *A. brasilense* Sp7 live cells [14,18] was modified to obtain extracellularly localised NPs of a more uniform size. Particularly, it is essential that, for the first time, the process of selenite reduction by bacterial cells was performed by adding SeO_3^{2-} not to the growing cells (e.g. in the beginning of the logarithmic growth phase, as was reported in virtually all the other relevant literature) but to the live bacterial biomass harvested after the logarithmic growth phase and in the beginning of the stationary growth phase (with the culture medium components removed by washing), suspended in sterile saline solution. In this case, the culture acquired a reddish tint (evidencing selenite reduction to red Se^0 NPs) already visible after 4 h and became pronouncedly red after 24 h (in contrast to our previous data where the reddish tint in a growing culture in contact with selenite appeared much later [18]).

FTIR spectroscopy is a well established highly informative analytical technique which has been successfully used in microbiology (see, e.g. relevant reviews [24–29] and recent representative experimental reports [30–33]). In our earlier related studies (see, e.g. Refs. [34–39]), FTIR spectroscopy was used to monitor changes on the molecular level in the structure and composition of cellular

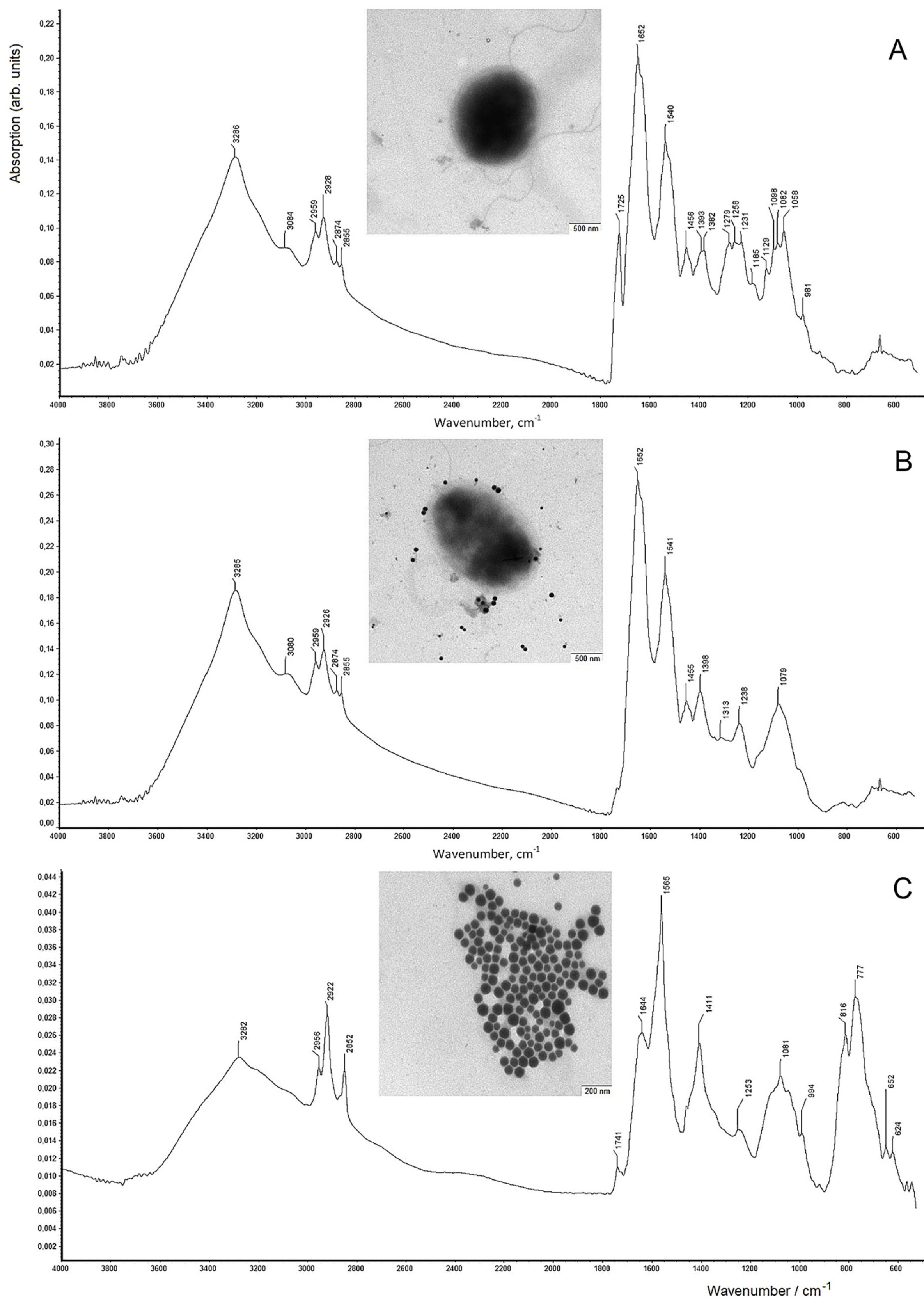

Fig. 1. Fourier transform infrared spectra (in the transmission mode, measured as dry biomass on ZnSe discs) of *Azospirillum brasilense* Sp7 harvested at the end of the logarithmic growth phase, separated by centrifugation, washed with saline solution and incubated at 32 °C for 24 h in saline without (A; control) and with 10 mM Na_2SeO_3 (B), as well as SeNPs synthesized therein (in sample B), separated from the cells and purified (C). Insets show typical transmission electron microscopic (TEM) images of the corresponding cells (in A, B; bars 500 nm) and Se NPs (in C; bar 200 nm).

Table 1
Wavenumbers of the main bands in the FTIR spectra (see Fig. 1) and their tentative assignment [25–29,38,40–42].

Sample	Tentative assignment of main bands to the relevant functional groups (wavenumbers, cm^{-1})															
	O–H; N–H (amide A in proteins), ν	C–H in $-CH_3$, ν_{as}	C–H in $>CH_2$, ν_{as}	C–H in $-CH_3$, ν_s	C–H in $>CH_2$, ν_s	C=O (ester moiety), ν	Amide I (in proteins)[a]	Carboxyl COO^-, ν_{as}	Amide II (in proteins)	$-CH_3$, δ (in proteins, lipids, polyesters, *etc.*)	COO^-, ν_s	C–O–C/ C–C–O ν (in ester moieties)	Amide III/ O–P=O ν_{as}	C–O, C–C ν, C–O–H, C–O–C δ in polysaccharides and polyesters	Phosphoryl groups, ν_s	COO^- δ; "fingerprint region"
Control: cell biomass of *A. brasilense* Sp7	3286 3084	2959	2928	2874	2855	1725	1652	ov.	1540	1456 1382[c]	1393[b]	1279 1258	1231[c]	1129[d] 1098 1082 1058[d]	981	vw
Cell biomass of *A. brasilense* Sp7 + 10 mM Na_2SeO_3	3285 3080	2959	2926	2874	2855	~1740 (sh)[e]	1652	ov.	1541	1455	1398[b]	–	1238	1079	sh	vw
Se NPs	3282 ~3080 (sh)	2956	2922	ov.	2852	1741	1644	1565	ov.	sh	1411	–	1253	1081	–	816 777

Designations: ν – stretching vibrations; ν_s – symmetric stretching vibrations; ν_{as} – antisymmetric stretching vibrations; δ – bending vibrations; sh – shoulder; vw – very weak; dash (–) means the absence of a band; ov. – a possible similar band is evidently overlapped by a neighbouring stronger one.

[a] The registered wavenumbers of amide I (in proteins) correspond to a dominating α-helix in bacterial cells in both cases and to a disordered secondary structure in Se NPs [25–27,38,40,41].

[b] May also be overlapped by ν(C–N) vibrations in cellular biomolecules.

[c] This band is partially overlapped by the neighbouring absorption bands of poly-3-hydroxybutyrate (PHB) [38].

[d] Polyester bands (poly-3-hydroxybutyrate) [38].

[e] A very weak shoulder featuring common cellular polyesters (lipopolysaccharides and phospholipids).

macrocomponents that accompanied metabolic responses of different strains of *A. brasilense* (showing different adaptation capabilities and often different behaviour) to various unfavourable conditions.

Fig. 1 (A–C) shows FTIR spectra (registered in the transmission mode) of the control sample of *A. brasilense* Sp7 biomass (incubated in saline solution for 24 h) and that after 24 h of contact with 10 mM SeO_3^{2-}, as well as of the Se NPs produced thereby (separated and purified as described in the experimental section). Typical transmission electron microscopic (TEM) images of the corresponding cells and Se NPs are also presented in Fig. 1 as insets. Wavenumbers of the maxima for the main bands in the FTIR spectra are summarised in Table 1 together with their tentative assignment [25–29,38,40–42].

In the TEM image of cells of *A. brasilense* Sp7 incubated for 24 h with 10 mM selenite (Fig. 1B), Se nanostructures can be seen as mostly extracellular electron-dense spherical particles which are absent in the control (Fig. 1A). In the TEM image of the isolated Se NPs (Fig. 1C), it can be seen that they are spherical, of relatively uniform size, with diameters within ca. 50–100 nm. It has to be noted that, as can be seen in Fig. 1C, there is a thin greyish fairly transparent layer between all adjoining particles which can be attributed to surface-associated biopolymers (see below).

The FTIR spectrum of the control culture (see Fig. 1A) represents typical IR spectral regions of bacterial biomass (see Table 1). However, the well-resolved ester ν(C=O) band at 1725 cm^{-1} (its assignment is additionally confirmed by the presence of other polyester-related bands in the C–O–C/C–C–O stretching and bending regions at 1279 and within 1150–1050 cm^{-1}; see Table 1) shows that incubation of the control culture in saline solution (without nutrients) for 24 h was sufficient for the stressed bacteria to start synthesising and accumulating the reserve biopolyester, which in azospirilla is known [43,44] to be represented by the homopolymer, poly-3-hydroxybutyrate (PHB). In cultures grown without a stress which would induce the accumulation of polyesters, this region is commonly featured by a very weak, sometimes hardly visible absorption due to common cellular polyesters (lipopolysaccharides and phospholipids) [24–27,35,37,38]. However, under nutrient limitations (primarily, a lack of bound nitrogen), many bacteria (including *A. brasilense*) tend to accumulate large amounts (up to 70%–80% of dry cell mass, d.c.m.) of PHB as intracellular granules [37–39,43,44].

In the case of Fig. 1A, the relatively low amount of PHB (represented by the moderate band at 1725 cm^{-1}, which, according to our evaluation as reported earlier [39], corresponds to ca. 10%–15% of d.c.m. PHB) is evidently limited by the lack of carbon-containing nutrients in the culture medium (those available for this moderate PHB biosynthesis might well be represented by bacterial exopolysaccharides and lysed cell components). It has also to be noted that the relatively low frequency of the PHB ν(C=O) band (1725 cm^{-1}), which is sensitive to the degree of PHB crystallisation (commonly appearing at higher wavenumbers, up to ca. 1750 cm^{-1}, in amorphous biopolyester, including that in bacterial cells) [45,46], shows that the sample preparation procedure used in our work (grinding of the dry biomass and drying at 45°C in a thin layer) could evidently promote intracellular PHB crystallisation.

It is of interest that under similar conditions (incubation of *A. brasilense* Sp7 for 24 h in saline solution), but in the presence of 10 mM SeO_3^{2-}, there are virtually no spectroscopic signs of PHB accumulation (see Fig. 1B), and the spectrum is fairly typical of Gram-negative bacteria. It can be reasoned that the moderate toxicity stress (induced by this concentration of selenite) switched the bacterial metabolism to reducing selenium(IV) to Se^0 (with the formation of Se NPs) without noticeable PHB biosynthesis. (Note that, while isolated Se NPs formed therein

gave a specific FTIR spectrum shown in Fig. 1C, the relative amount of Se NPs in the bacterial culture corresponding to Fig. 1B was too low to give any appreciable spectroscopic contribution specifically from Se NPs.)

The FTIR spectrum of isolated Se NPs (see Fig. 1C) differs substantially from those of the bacterial cultures. Nevertheless, the typical protein bands, amide I (at 1644 cm^{-1}) and low-intensity amide III (at 1253 cm^{-1}) can be clearly seen, The typical amide II band of proteins (at about 1540 cm^{-1}) in this case is evidently overlapped by the very strong carboxylate band $\nu_{as}(COO^-)$ at 1565 cm^{-1}, which is accompanied by the strong $\nu_s(COO^-)$ band at 1411 cm^{-1} (evidently also contributing with the $\delta(COO^-)$ modes to the fingerprint region below ca. 850 cm^{-1}). Note that all the relevant carboxyl bands in the spectra of cells (Fig. 1A and B), which may naturally correspond to amino acid side-chains of cellular proteins and/or to carboxypolysaccharides, are either overlapped by neighbouring stronger bands or significantly lower in intensity (see Table 1). Typical polysaccharide vibration region (within 1200–950 cm^{-1}) is also featured by prominent absorption (see Fig. 1C). This clearly shows the presence of proteins and polysaccharides in the biomacromolecules capping the Se NPs surface, in line with the TEM image (see inset in Fig. 1C) and with the literature on biosynthesised Se nanostructures [4,5,19,20,47–50]. The lower frequency of the amide I band (1644 cm^{-1}) of the proteins capping the Se NPs, as compared to that of cellular proteins (1652 cm^{-1}; see Table 1), suggests that the secondary structure of the proteins in the bacterial cells represented by dominating α-helix [25–27,38,40,41] differs from the evidently disordered secondary structure of the proteins capping the surface of Se NPs.

It has to be emphasised that the evident abundance of carboxylic groups, featured by prominent bands (see above and Table 1), in the biopolymers capping the Se NPs contributes to their stability in suspension by governing their surface charge [19]. This is corroborated by the negative zeta-potentials of biogenic Se NPs reported in the literature in circumneutral media [19,50]; also our recent measurements of zeta-potential of Se NPs similarly produced by another strain, *A. brasilense* Sp245 [14,18], showed the range −(21 … 24) mV (A.V. Tugarova, P.V. Mamchenkova, A.A. Kamnev, unpublished results).

Finally, we would like to mention that within the region of stretching ν(C–H) vibrations (3000–2800 cm^{-1}), biopolymers associated with Se NPs show significantly higher intensities of the $\nu(CH_2)$ bands at 2922 and 2852 cm^{-1} than those of the $\nu(CH_3)$ bands (see Fig. 1C and Table 1), as compared to this region in bacterial cells (see Fig. 1A and B and Table 1). Such an increase in the relative intensity of $-CH_2-$ vibrations (vs. those of $-CH_3$) can be related to the presence of lipids (featured by aliphatic chains of fatty acid residues) in the capping layer of the Se NPs (this assumption is also corroborated by the appearance of the ν(C═O) ester carbonyl band, typical of lipids, at 1741 cm^{-1}; see Fig. 1C). Note that lipids have recently been reported to be among biopolymeric capping constituents of microbially produced Se NPs [49].

While the aforementioned spectroscopic distinctions may logically represent differences in the molecular composition between cellular biomolecules and those associated with the Se NPs, some possibility for a redistribution of the FTIR spectral intensities owing to surface-enhancement effects (similar to those observed, e.g. on gold nanoparticles [51–53] due to localised surface plasmon resonance effects, with the relevant surface selection rules), observed for the Se NPs, cannot be excluded. This, however, requires special experiments on the possibility of such IR spectroscopic 'surface exciton resonance' effects for semiconductor selenium NPs which evidently lack such free conductivity electrons (plasmon) as in noble metals.

4. Conclusions

Extracellular Se NPs relatively homogeneous in size (with average diameters within 50–100 nm) were obtained in the process of selenite reduction by live biomass of the rhizobacterium *A. brasilense* Sp7 (harvested after the logarithmic growth phase and washed from culture medium components). Both the control cultures of *A. brasilense* Sp7 and those incubated with SeO_3^{2-} (producing Se NPs), as well as the resulting separated Se NPs were studied using FTIR spectroscopy in the transmission mode (measured as dried layers on a ZnSe disc), in addition to TEM, to compare metabolic changes in cells and the bioorganic layers associated with the Se NPs. In the control culture (stored for 24 h in physiological saline), FTIR spectroscopic signs of poly-3-hydroxybutyrate (a 'reserve' biopolyester) were observed as a response to the lack of nutrients (trophic stress), whereas they were virtually absent in cells incubated for 24 h in physiological saline with 10 mM SeO_3^{2-} (toxicity stress). FTIR spectra of Se NPs separated from bacterial cells showed bands typical of proteins, polysaccharides and lipids associated with the particles (in line with their TEM images showing a thin layer over the particles), in addition to strong carboxylate bands, which evidently stabilise the NP structure and morphology.

Conflict of interest statement

The authors declare that the research was conducted in the absence of any commercial or financial relationships that could be construed as a potential conflict of interest.

Acknowledgements

In this study, experiments were performed in part on the equipment of the "Simbioz" Centre for the Collective Use of Research Equipment in the field of physical–chemical biology and nanobiotechnology at IBPPM RAS, Saratov, Russia (Zetasizer Nano-ZS, FTIR spectrometer Nicolet 6700, transmission electron microscope Libra-120). The main materials of this paper were presented in a sectional talk at the 33rd European Congress on Molecular Spectroscopy (EUCMOS-2016; 30 August–4 September 2016, Szeged, Hungary); A.A.K. acknowledges the support provided by the EUCMOS-2016 Organising Committee for participating in the Congress. The authors are grateful to Dr. A.M. Burov (this Institute, Saratov, Russia) for his help in carrying out the transmission electron microscopic experiments. Thanks are also due to E.A. Polivoda and A.A. Budanova (this Institute, Saratov, Russia) for their technical assistance with transmission electron microscopy. This study was supported in part by The Russian Foundation for Basic Research (Grant 16-08-01302-a).

References

[1] K.B. Narayanan, N. Sakthivel, Biological synthesis of metal nanoparticles by microbes, Adv. Coll. Interface Sci. 156 (1) (2010) 1–13, http://dx.doi.org/10.1016/j.cis.2010.02.001.
[2] A. Husen, K.S. Siddiqi, Plants and microbes assisted selenium nanoparticles: characterization and application, J. Nanobiotechnol. 12 (2014) 28, http://dx.doi.org/10.1186/s12951-014-0028-6.
[3] M. Durán, C.P. Silveira, N. Durán, Catalytic role of traditional enzymes for biosynthesis of biogenic metallic nanoparticles: a mini-review, IET Nanobiotechnol. 9 (5) (2015) 314–323, http://dx.doi.org/10.1049/iet-nbt.2014.0054.
[4] S. Shirsat, A. Kadam, Mu. Naushad, R.S. Mane, Selenium nanostructures: microbial synthesis and applications, RSC Adv. 5 (112) (2015) 92799–92811, http://dx.doi.org/10.1039/C5RA17921A.
[5] S.A. Wadhwani, U.U. Shedbalkar, R. Singh, B.A. Chopade, Biogenic selenium nanoparticles: current status and future prospects, Appl. Microbiol. Biotechnol. 100 (6) (2016) 2555–2566, http://dx.doi.org/10.1007/s00253-016-7300-7.

[6] S. Chaudhary, S.K. Mehta, Selenium nanomaterials: applications in electronics, catalysis and sensors, J. Nanosci. Nanotechnol. 14 (2) (2014) 1658–1674, http://dx.doi.org/10.1166/jnn.2014.9128.

[7] S. Chaudhary, A. Umar, S.K. Mehta, Surface functionalized selenium nanoparticles for biomedical applications, J. Biomed. Nanotechnol. 10 (10) (2014) 3004–3042, http://dx.doi.org/10.1166/jbn.2014.1985.

[8] A.S. Eswayah, T.J. Smith, P.H.E. Gardiner, Microbial transformations of selenium species of relevance to bioremediation, Appl. Environ. Microbiol. 82 (16) (2016) 4848–4859, http://dx.doi.org/10.1128/AEM.00877-16.

[9] S. Skalickova, V. Milosavljevic, K. Cihalova, P. Horky, L. Richtera, V. Adam, Selenium nanoparticles as a nutrition supplement, Nutrition 33 (2017) 83–90, http://dx.doi.org/10.1016/j.nut.2016.05.001.

[10] P. Vera, Y. Echegoyen, E. Canellas, C. Nerin, M. Palomo, Y. Madrid, C. Cámara, Nano selenium as antioxidant agent in a multilayer food packaging material, Anal. Bioanal. Chem. 408 (24) (2016) 6659–6670, http://dx.doi.org/10.1007/s00216-016-9780-9.

[11] L. Simon, B. Biró, É. Széles, S. Balázsy, Szelén fitoextrakciója és mikrobacsoportok előfordulása szennyezett talajokban (“Phytoextraction of selenium and occurrence of microbial groups in contaminated soils”, in Hungarian), Agrokém. Talajt. 56 (1) (2007) 161–172, http://dx.doi.org/10.1556/Agrokem.56.2007.1.12.

[12] G.M. Gadd, Metals, minerals and microbes: geomicrobiology and bioremediation, Microbiology 156 (3) (2010) 609–643, http://dx.doi.org/10.1099/mic.0.037143-0.

[13] A.V. Tugarova, A.M. Burov, M.M. Burashnikova, A.A. Kamnev, Gold(III) reduction by the rhizobacterium *Azospirillum brasilense* with the formation of gold nanoparticles, Microb. Ecol. 67 (1) (2014) 155–160, http://dx.doi.org/10.1007/s00248-013-0329-6.

[14] A.V. Tugarova, E.P. Vetchinkina, E.A. Loshchinina, A.G. Shchelochkov, V.E. Nikitina, A.A. Kamnev, The ability of the rhizobacterium *Azospirillum brasilense* to reduce selenium(IV) to selenium(0), Microbiology (Moscow) 82 (3) (2013) 352–355, http://dx.doi.org/10.1134/S0026261713030120.

[15] Y. Bashan, L.E. de-Bashan, How the plant growth-promoting bacterium *Azospirillum* promotes plant growth – a critical assessment, Adv. Agron. 108 (2010) 77–136, http://dx.doi.org/10.1016/S0065-2113(10)08002-8.

[16] L. Pereg, L.E. de-Bashan, Y. Bashan, Assessment of affinity and specificity of *Azospirillum* for plants, Plant Soil 399 (1–2) (2016) 389–414, http://dx.doi.org/10.1007/s11104-015-2778-9.

[17] F. Cassán, M. Diaz-Zorita, *Azospirillum* sp. in current agriculture: from the laboratory to the field, Soil Biol. Biochem. 103 (2016) 117–130, http://dx.doi.org/10.1016/j.soilbio.2016.08.020.

[18] A.V. Tugarova, E.P. Vetchinkina, E.A. Loshchinina, A.M. Burov, V.E. Nikitina, A.A. Kamnev, Reduction of selenite by *Azospirillum brasilense* with the formation of selenium nanoparticles, Microb. Ecol. 68 (3) (2014) 495–503, http://dx.doi.org/10.1007/s00248-014-0429-y.

[19] R. Jain, N. Jordan, S. Weiss, H. Foerstendorf, K. Heim, R. Kacker, R. Hübner, H. Kramer, E.D. van Hullebusch, F. Farges, P.N.L. Lens, Extracellular polymeric substances govern the surface charge of biogenic elemental selenium nanoparticles, Environ. Sci. Technol. 49 (3) (2015) 1713–1720, http://dx.doi.org/10.1021/es5043063.

[20] S. Lampis, E. Zonaro, C. Bertolini, D. Cecconi, F. Monti, M. Micaroni, R.J. Turner, C.S. Butler, G. Vallini, Selenite biotransformation and detoxification by *Stenotrophomonas maltophilia* SeITE02: novel clues on the route to bacterial biogenesis of selenium nanoparticles, J. Hazard. Mater (2016), http://dx.doi.org/10.1016/j.jhazmat.2016.02.035.

[21] J.J. Tarrand, N.R. Krieg, J. Döbereiner, A taxonomic study of the *Spirillum lipoferum* group, with descriptions of a new genus, *Azospirillum* gen. nov. and two species, *Azospirillum lipoferum* (Beijerinck) comb. nov. and *Azospirillum brasilense* sp. nov, Can. J. Microbiol. 24 (8) (1978) 967–980, http://dx.doi.org/10.1139/m78-160.

[22] R. Gherna, P. Pienta, R. Cote, American Type Culture Collection. Catalogue of Bacteria and Phages, eighteenth ed., ATCC, Rockville, USA, 1992, p. 34.

[23] J.M. Day, J. Döbereiner, Physiological aspects of N_2-fixation by a *Spirillum* from *Digitaria* roots, Soil Biol. Biochem. 8 (1) (1976) 45–50, http://dx.doi.org/10.1016/0038-0717(76)90020-1.

[24] D. Naumann, S. Keller, D. Helm, Ch. Schultz, B. Schrader, FT-IR spectroscopy and FT-Raman spectroscopy are powerful analytical tools for the non-invasive characterization of intact microbial cells, J. Mol. Struct. 347 (1995) 399–405, http://dx.doi.org/10.1016/0022-2860(95)08562-A.

[25] D. Naumann, Infrared spectroscopy in microbiology, in: R.A. Meyers (Ed.), Encyclopedia of Analytical Chemistry, Wiley, Chichester, UK, 2000, pp. 102–131, http://dx.doi.org/10.1002/9780470027318.a0117 (Updated version: P. Lasch, D. Naumann. Infrared spectroscopy in microbiology. In: R.A. Meyers (ed.). Encyclopedia of Analytical Chemistry. J. Wiley & Sons. Published online 12 March 2015. DOI: 10.1002/9780470027318.a0117.pub2).

[26] M. Beekes, P. Lasch, D. Naumann, Analytical applications of Fourier transform-infrared (FT-IR) spectroscopy in microbiology and prion research, Vet. Microbiol. 123 (4) (2007) 305–319, http://dx.doi.org/10.1016/j.vetmic.2007.04.010.

[27] A.A. Kamnev, FTIR spectroscopic studies of bacterial cellular responses to environmental factors, plant-bacterial interactions and signalling, Spectrosc. Int. J. 22 (2–3) (2008) 83–95, http://dx.doi.org/10.3233/SPE-2008-0329.

[28] A. Alvarez-Ordonez, D.J.M. Mouwen, M. Lopez, M. Prieto, Fourier transform infrared spectroscopy as a tool to characterize molecular composition and stress response in foodborne pathogenic bacteria, J. Microbiol. Methods 84 (3) (2011) 369–378, http://dx.doi.org/10.1016/j.mimet.2011.01.009.

[29] J.J. Ojeda, M. Dittrich, Fourier transform infrared spectroscopy for molecular analysis of microbial cells, in: A. Navid (Ed.), Microbial Systems Biology: Methods and Protocols (Methods in Molecular Biology, vol. 881), Chapter 8, Springer Science+Business Media, LLC, 2012, pp. 187–211, http://dx.doi.org/10.1007/978-1-61779-827-6_8.

[30] C. Saulou, F. Jamme, L. Girbal, C. Maranges, I. Fourquaux, M. Cocaign-Bousquet, P. Dumas, M. Mercier-Bonin, Synchrotron FTIR microspectroscopy of *Escherichia coli* at single-cell scale under silver-induced stress conditions, Anal. Bioanal. Chem. 405 (8) (2013) 2685–2697, http://dx.doi.org/10.1007/s00216-013-6725-4.

[31] E. Skotti, S. Kountouri, P. Bouchagier, D.I. Tsitsigiannis, M. Polissiou, P.A. Tarantilis, FTIR spectroscopic evaluation of changes in the cellular biochemical composition of the phytopathogenic fungus *Alternaria alternata* induced by extracts of some Greek medicinal and aromatic plants, Spectrochim. Acta Part A Mol. Biomol. Spectrosc. 127 (2014) 463–472, http://dx.doi.org/10.1016/j.saa.2014.02.113.

[32] I. Ferreira, J. Ferreira-Strixino, M.L. Castilho, C.B.L. Campos, C. Tellez, L. Raniero, Characterization of *Paracoccidioides brasiliensis* by FT-IR spectroscopy and nanotechnology, Spectrochim. Acta Part A Mol. Biomol. Spectrosc. 152 (2016) 397–403, http://dx.doi.org/10.1016/j.saa.2015.07.061.

[33] A. Spence, B.P. Kelleher, Photodegradation of major soil microbial biomolecules is comparable to biodegradation: insights from infrared and diffusion editing NMR spectroscopies, J. Mol. Struct. 1107 (2016) 7–13, http://dx.doi.org/10.1016/j.molstruc.2015.11.025.

[34] A.A. Kamnev, M. Ristić, L.P. Antonyuk, A.V. Chernyshev, V.V. Ignatov, Fourier transform infrared spectroscopic study of intact cells of the nitrogen-fixing bacterium *Azospirillum brasilense*, J. Mol. Struct. 408/409 (1997) 201–205, http://dx.doi.org/10.1016/S0022-2860(96)09532-4.

[35] A.A. Kamnev, L.P. Antonyuk, A.V. Tugarova, P.A. Tarantilis, M.G. Polissiou, P.H.E. Gardiner, Fourier transform infrared spectroscopic characterisation of heavy metal-induced metabolic changes in the plant-associated soil bacterium *Azospirillum brasilense* Sp7, J. Mol. Struct. 610 (1–3) (2002) 127–131, http://dx.doi.org/10.1016/S0022-2860(02)00021-2.

[36] A.A. Kamnev, L.P. Antonyuk, L.Yu. Matora, O.B. Serebrennikova, M.V. Sumaroka, M. Colina, M.-F. Renou-Gonnord, V.V. Ignatov, Spectroscopic characterization of cell membranes and their constituents of the plant-associated soil bacterium *Azospirillum brasilense*, J. Mol. Struct. 480–481 (1999) 387–393, http://dx.doi.org/10.1016/S0022-2860(98)00712-1.

[37] A.A. Kamnev, A.V. Tugarova, L.P. Antonyuk, P.A. Tarantilis, L.A. Kulikov, Yu.D. Perfiliev, M.G. Polissiou, P.H.E. Gardiner, Instrumental analysis of bacterial cells using vibrational and emission Mössbauer spectroscopic techniques, Anal. Chim. Acta 573–574 (2006) 445–452, http://dx.doi.org/10.1016/j.aca.2006.04.041.

[38] A.A. Kamnev, J.N. Sadovnikova, P.A. Tarantilis, M.G. Polissiou, L.P. Antonyuk, Responses of *Azospirillum brasilense* to nitrogen deficiency and to wheat lectin: a diffuse reflectance infrared Fourier transform (DRIFT) spectroscopic study, Microb. Ecol. 56 (4) (2008) 615–624, http://dx.doi.org/10.1007/s00248-008-9381-z.

[39] A.A. Kamnev, A.V. Tugarova, P.A. Tarantilis, P.H.E. Gardiner, M.G. Polissiou, Comparing poly-3-hydroxybutyrate accumulation in *Azospirillum brasilense* strains Sp7 and Sp245: the effects of copper (II), Appl. Soil Ecol. 61 (2012) 213–216, http://dx.doi.org/10.1016/j.apsoil.2011.10.020.

[40] D. Naumann, FT-infrared and FT-Raman spectroscopy in biomedical research, Appl. Spectrosc. Rev. 36 (2–3) (2001) 239–298, http://dx.doi.org/10.1081/ASR-100106157.

[41] A. Barth, Infrared spectroscopy of proteins, Biochim. Biophys. Acta 1767 (9) (2007) 1073–1101, http://dx.doi.org/10.1016/j.bbabio.2007.06.004.

[42] Z. Movasaghi, S. Rehman, I. ur Rehman, Fourier transform infrared (FTIR) spectroscopy of biological tissues, Appl. Spectrosc. Rev. 43 (2) (2008) 134–179, http://dx.doi.org/10.1080/05704920701829043.

[43] R. Itzigsohn, O. Yarden, Y. Okon, Polyhydroxyalkanoate analysis in *Azospirillum brasilense*, Can. J. Microb. 41 (Suppl. 1) (1995) 73–76, http://dx.doi.org/10.1139/m95-171.

[44] D. Kadouri, E. Jurkevitch, Y. Okon, Involvement of the reserve material poly-β-hydroxybutyrate in *Azospirillum brasilense* stress endurance and root colonization, Appl. Environ. Microbiol. 69 (6) (2003) 3244–3250, http://dx.doi.org/10.1128/AEM.69.6.3244-3250.2003.

[45] M. Kansiz, A. Domínguez-Vidal, D. McNaughton, B. Lendl, Fourier-transform infrared (FTIR) spectroscopy for monitoring and determining the degree of crystallisation of polyhydroxyalkanoates (PHAs), Anal. Bioanal. Chem. 388 (5) (2007) 1207–1213, http://dx.doi.org/10.1007/s00216-007-1337-5.

[46] H. Sato, R. Murakami, K. Mori, Y. Ando, I. Takahashi, I. Noda, Y. Ozaki, Specific crystal structure of poly(3-hydroxybutyrate) thin films studied by infrared reflection–absorption spectroscopy, Vibr. Spectrosc. 51 (1) (2009) 132–135, http://dx.doi.org/10.1016/j.vibspec.2008.11.010.

[47] J. Dobias, E.I. Suvorova, R. Bernier-Latmani, Role of proteins in controlling selenium nanoparticle size, Nanotechnology 22 (19) (2011) 195605, http://dx.doi.org/10.1088/0957-4484/22/19/195605.

[48] S.I. Yang, G.N. George, J.R. Lawrence, S.G.W. Kaminskyj, J.J. Dynes, B. Lai, I.J. Pickering, Multispecies biofilms transform selenium oxyanions into elemental selenium particles: studies using combined synchrotron X-ray fluorescence imaging and scanning transmission X-ray microscopy, Environ. Sci. Technol. (2016), http://dx.doi.org/10.1021/acs.est.5b04529.

[49] G. Gonzalez-Gil, P.N.L. Lens, P.E. Saikaly, Selenite reduction by anaerobic

microbial aggregates: microbial community structure, and proteins associated to the produced selenium spheres, Front. Microbiol. 7 (2016), http://dx.doi.org/10.3389/fmicb.2016.00571. Article 571(14 pp.).
[50] N. Mollania, R. Tayebee, F. Narenji-Sani, An environmentally benign method for the biosynthesis of stable selenium nanoparticles, Res. Chem. Intermed. 42 (5) (2016) 4253–4271, http://dx.doi.org/10.1007/s11164-015-2272-2.
[51] A.A. Kamnev, L.A. Dykman, P.A. Tarantilis, M.G. Polissiou, Spectroimmunochemistry using colloidal gold bioconjugates, Biosci. Rep. 22 (5–6) (2002) 541–547, http://dx.doi.org/10.1023/A:1022077920527.
[52] K. Ataka, J. Heberle, Biochemical applications of surface-enhanced infrared absorption spectroscopy, Anal. Bioanal. Chem. 388 (1) (2007) 47–54, http://dx.doi.org/10.1007/s00216-006-1071-4.
[53] I.A. Larmour, D. Graham, Surface enhanced optical spectroscopies for bioanalysis, Analyst 136 (19) (2011) 3831–3853, http://dx.doi.org/10.1039/c1an15452d.